the plant journal

SEB SOCIETY FOR EXPERIMENTAL BIOLOGY

The Plant Journal (2022) **109,** 1386–1396 doi: 10.1111/tpj.15636

Cyclic nucleotide-gated ion channel 6 is involved in extracellular ATP signaling and plant immunity

Ha N. Duong[1,†], Sung-Hwan Cho[1,†], Limin Wang[2], An Q. Pham[1,‡], Julia M. Davies[2] and Gary Stacey[1,*]

[1]*Divisions of Plant Sciences and Technology and Biochemistry, National Center for Soybean Biotechnology, Christopher S. Bond Life Sciences Center, University of Missouri, Columbia, MO 65211, USA, and*

[2]*Department of Plant Sciences, University of Cambridge, Cambridge CB2 3EA, UK*

Received 10 September 2021; revised 5 December 2021; accepted 9 December 2021; published online 16 December 2021.

*For correspondence (e-mail staceyg@missouri.edu).

†These authors contributed equally to this work.

‡Present address: Faculty of Biology and Biotechnology, VNUHCM-University of Sciences, Hochiminh, Vietnam

SUMMARY

Extracellular ATP (eATP) is known to act as a danger signal in both plants and animals. In plants, eATP is recognized by the plasma membrane (PM)-localized receptor P2K1 (LecRK-I.9). Among the first measurable responses to eATP addition is a rapid rise in cytoplasmic free calcium levels ($[Ca^{2+}]_{cyt}$), which requires P2K1. However, the specific transporter/channel proteins that mediate this rise in $[Ca^{2+}]_{cyt}$ are unknown. Through a forward genetic screen, we identified an Arabidopsis ethylmethanesulfonate (EMS) mutant impaired in the $[Ca^{2+}]_{cyt}$ response to eATP. Positional cloning revealed that the mutation resided in the *cngc6* gene, which encodes cyclic nucleotide-gated ion channel 6 (CNGC6). Mutation of the *CNGC6* gene led to a notable decrease in the PM inward Ca^{2+} current in response to eATP. eATP-induced mitogen-activated protein kinase activation and gene expression were also significantly lower in *cngc6* mutant plants. In addition, *cngc6* mutant plants were also more susceptible to the bacterial pathogen *Pseudomonas syringae*. Taken together, our results indicate that CNGC6 plays a crucial role in mediating eATP-induced $[Ca^{2+}]_{cyt}$ signaling, as well as plant immunity.

Keywords: extracellular ATP, cyclic nucleotide-gated ion channel 6, CNGC6, cytosolic calcium, plant immunity.

INTRODUCTION

ATP is well known as the energy molecule driving essential biochemical reactions within living organisms. Inside the cell, the ATP concentration is kept at a high level (in the mM range) while the extracellular concentration is significantly lower (in the nM–μM range) (Gout et al., 1992; Yegutkin et al., 2006). However, at this concentration, extracellular ATP (eATP) acts as a potent extracellular signal, as has been demonstrated in both plants and animals (Cekic and Linden, 2016; Cho et al., 2017; Khakh and Burnstock, 2009; Tanaka et al., 2014). ATP can be released to the extracellular matrix through wounding (Song et al., 2006), exocytosis (Kim et al., 2006), or active transport, where it is subsequently recognized by specific plasma membrane (PM)-localized receptors (Burnstock, 2006a).

The eATP signaling (i.e., purinergic signaling) pathway in animals is well studied with extensive medical implications. For example, the mammalian P2X7 receptor is the most extensively studied from an immunological perspective and is involved in both innate and adaptive immune responses (Savio et al., 2018). eATP participates in a broad range of animal physiological functions among; for example, it serves as a danger signal during pathogen infection or wounding (Rhett et al., 2014; van der Vliet and Bove, 2011). As such, eATP is considered a damage-associated molecular pattern (DAMP). Animals perceive eATP through two groups of receptors: ligand-gated ion channels (P2Xs) and G-coupled protein receptors (P2Ys) (Burnstock, 2006b). One of the earliest cellular changes upon binding of eATP to these receptors is the elevation of the cytosolic free calcium concentration ($[Ca^{2+}]_{cyt}$), followed by an increase in the levels of reactive oxygen species (ROS) and nitric oxide (NO) (Dichmann et al., 2000; Silva et al., 2006).

Relative to the rich research literature on eATP function in animals, very little is known about the functional roles of eATP in plants. However, similar to animals, a number of papers have implicated eATP in a variety of plant physiological processes, including the response to pathogen infection (Pham et al., 2020), the response to wounding (Choi et al., 2014), thigmotropism (Weerasinghe et al.,

2009), pollen growth (Wu et al., 2018), and root hair development (Clark and Roux, 2018), among others (Cho et al., 2017; Tanaka et al., 2010a). In addition, eATP is involved in root gravitropism through polar auxin transport (Tang et al., 2003) and modulates root skewing as well (Yang et al., 2015). As is the case in animals, eATP functions as a DAMP in plants with similar initial cellular responses; for example, eATP addition leads to a rapid change in $[Ca^{2+}]_{cyt}$ (Cho et al., 2017; Clark et al., 2010; Demidchik et al., 2009; Kim et al., 2006; Song et al., 2006; Tanaka et al., 2010b), as well as an elevation of ROS levels (Chen et al., 2017). However, unlike animals, plants appear to lack canonical P2X or P2Y receptors. In 2014, through a forward genetic screening approach, the first plant eATP receptor was isolated and identified as a PM-localized L-type lectin receptor-like kinase (LecRK-I.9), which was originally termed DORN1 but subsequently renamed P2K1 to align the plant nomenclature with that of animal purinoreceptors (Choi et al., 2014).

The identification of P2K1 has led to a significant increase in our knowledge of the molecular events surrounding plant purinergic signaling. For example, Chen et al. (2017) showed that eATP induces stomatal immunity against *Pseudomonas syringae* through P2K1-mediated activation of the NADPH oxidase RBOHD. Protein acyltransferases such as PAT5 and PAT9 were found to be phosphorylated by P2K1, which in turn mediated the eATP response by *S*-acylation of P2K1 (Chen et al., 2021). In addition, several studies indicated crosstalk between eATP and jasmonate (JA) signaling for plant defense responses (Balague et al., 2017; Jewell et al., 2019; Tripathi et al., 2018). eATP enhances the interaction between the JA receptor coronatine-insensitive 1 (COI1) and a key suppressor of JA signaling, ZIM-domain 1 (JAZ1), and elevates plant defense against pathogens (Tripathi et al., 2018). P2K1 is required for pathogen resistance through the regulation of JA signaling components (Balague et al., 2017). eATP-induced defense-related gene expression mediated by P2K1 requires CAMTA3 and the MYC transcription factor (Jewell et al., 2019). Animals possess multiple P2X and P2Y receptors, consistent with the broad role of purinergic signaling. Hence, it was notable that a second plant eATP receptor, P2K2, was recently discovered (Pham et al., 2020). P2K2 is strongly expressed under stress conditions, interacts directly with P2K1, and is also involved in plant defense to invading pathogens.

Calcium (Ca^{2+}) plays an important role as a secondary messenger with increased $[Ca^{2+}]_{cyt}$ levels induced by various biotic and abiotic stresses (Dodd et al., 2010; Kudla et al., 2010). For example, a key feature of DAMP-mediated responses is the transient opening of PM calcium channels, admitting an inward flux of calcium from the extracellular space (Choi et al., 2014; Pham et al., 2020). For calcium to function as an intracellular signal, stimulus-specific changes in cytoplasmic levels need to be precisely regulated (McAinsh and Pittman, 2009). Calcium ion influx into plant cells is mainly accomplished by non-selective calcium channels, depolarization-activated calcium channels, and hyperpolarization-activated calcium channels (HACCs) (Demidchik et al., 2018; Lemtiri-Chlieh et al., 2020; Very and Sentenac, 2002; White and Broadley, 2003). For example, patch-clamp electrophysiology analysis detected the activity of HACCs in response to eATP in plants (Demidchik et al., 2009; Wang et al., 2014, 2018; Wu and Wu, 2008). The family of annexins, glutamate receptor-like (GLR) channels, and cyclic-nucleotide-gated channels (CNGCs), which were previously predicted or shown to have HACC activity, have been suggested as potential candidates mediating $[Ca^{2+}]_{cyt}$ changes in response to eATP (Matthus et al., 2020; Wang et al., 2019). For example, ANNEXIN1 underpins the hydroxyl radical-activated HACC in mature epidermis and root hairs (Laohavisit et al., 2012). This annexin was subsequently suggested to play a role in eATP-induced Ca^{2+} elevation (Mohammad-Sidik et al., 2021). However, since loss of ANNEXIN1 did not completely abolish the $[Ca^{2+}]_{cyt}$ response to eATP, other calcium channels are likely required. Two GLRs, GLR3.3 and GLR3.6, were shown to mediate $[Ca^{2+}]_{cyt}$ increases triggered by wounding (Vincent et al., 2017). In addition, patch-clamp analyses implicated several Arabidopsis CNGCs, such as CNGC2, CNGC4, CNGC5, and CNGC6, in HACC conductances (Gao et al., 2012; Tian et al., 2019; Wang et al., 2013). Most recently, CNGC2 and CNGC4 were reported to be involved in eATP-regulated pollen germination, pollen tube growth, and ion flux (Wu et al., 2021).

In order to identify genes involved in plant purinergic signaling and, specifically, in the $[Ca^{2+}]_{cyt}$ response to eATP, we conducted a forward genetic screen in which aequorin luminescence was used to measure the plant cellular response. Among the mutants identified in this screen was one in which the *CNGC6* gene was mutated, resulting in a significant reduction in the normal elevation of $[Ca^{2+}]_{cyt}$ seen upon eATP addition. Intriguingly, CNGC6 has been previously shown to form a conductive Ca^{2+}-permeable channel in the root cell PM, as well as when heterologously expressed in HEK293T cells (Gao et al., 2012; Tan et al., 2020). In the current study, patch-clamp analyses showed that *cngc6* mutant plants were defective in the PM inward Ca^{2+} current in response to eATP. These mutant plants were also found to be defective in the activation of mitogen-activated protein kinase (MAPK) and gene transcription normally associated with a response to eATP. As is the case for *p2k1* mutant plants, *cngc6* mutant plants were also significantly more susceptible to bacterial pathogen infection. These data implicate CNGC6 as a key calcium channel protein involved in the early events of plant purinergic signaling.

RESULTS

367 mutant plants are impaired in the $[Ca^{2+}]_{cyt}$ response to extracellular nucleotides

We generated an ethylmethanesulfonate (EMS)-mutagenized *Arabidopsis thaliana* library and carried out a similar screen to that reported previously by Choi et al. (2014) to identify mutants defective in the cellular calcium response to added eATP. Following the strategy in Figure S1, we screened approximately 30 000 M_0 generation plants, which led to the identification of mutant *367* showing a significant reduction in $[Ca^{2+}]_{cyt}$ elevation upon eATP elicitation (Figure 1a). To see whether *367* mutant plants showed a specific response to purine nucleotides, we tested the calcium response of *367* mutant plants to a variety of nucleotides. *367* mutant plants showed defects in the $[Ca^{2+}]_{cyt}$ response to various nucleotides, such as CTP, GTP, ITP, and UTP, compared with wild-type plants (Figure 1b). In contrast, the $[Ca^{2+}]_{cyt}$ response of the *367* mutant plants to different abiotic and biotic elicitors was similar to those of wild-type plants, except for chitin (Figure 1c,d). The latter may be due to the fact that chitin is known to cause the release of eATP (Kim et al., 2006). In addition, the *367* mutant plants exhibited a slighty lighter color and a weak-lobed leaf shape in comparison with wild-type (Col-0) plants at the 4-week-old stage (Figure S4).

To assess whether the lack of a $[Ca^{2+}]_{cyt}$ response to nucleotides in *367* mutant plants is controlled by a single gene, we crossed M_3 generation mutant plants with wild-type Col-0 and observed the segregation in F_2 progeny. The lack of a $[Ca^{2+}]_{cyt}$ response to ATP was found in 25% of the progeny (12 mutants:43 wild-type plants, $\chi^2 = 0.69$, d.f. = 1, $P_{0.05} = 3.84$), indicating a 3:1 ratio of a recessive gene, following Mendelian single gene inheritance.

The phenotype of the *367* mutant is due to disruption in the gene encoding CNGC6

In order to identify the gene responsible for the *367* mutant phenotype, we performed map-based cloning and whole-genome sequencing (WGS). We were able to map the *367* mutation to a 3.6-Mbp interval on chromosome 2 (Figure 2a; Table S1). Subsequent WGS found four genes with point mutations within this region (Figure 2a; Table S2). To confirm which mutation was responsible for the *367* mutant phenotype, we cloned each of these four genes individually and tested their ability to complement the *367* mutant phenotype. These experiments showed that only wild-type *CNGC6* driven by the *CNGC6* native promoter rescued the ATP-induced $[Ca^{2+}]_{cyt}$ influx response in *367* mutant plants (Figure 2c,d; Figure S3). The mutation of the *CNGC6* gene in the 367 mutant results in an early stop codon caused by a single nucleotide substitution (TGG → TGA, W661stop) within the highly conserved domain known to be critical for CNGC channel function (Figure 2a,b). Subsequently, we obtained the *cngc6* T-DNA mutant, *cngc6-1*, which was also found to be defective in the eATP-induced $[Ca^{2+}]_{cyt}$ response (Figure S2a). The F_1 progeny obtained from the cross between *cngc6-1* and *367* mutant plants were also defective in the ATP-induced $[Ca^{2+}]_{cyt}$ response, which indicates allelism (Figure S2c). Overall, these results indicate that the phenotype of the *367* mutant plants is the result of a mutation in *CNGC6*. Therefore, we denote the *367* mutation as *cngc6-3*, following the published allele (Gao et al., 2012; Wang et al., 2013).

eATP-induced current activation does not occur in *cngc6* mutant plants

CNGC6 was previously reported as a PM-localized Ca^{2+}-permeable channel responsible for plant responses to heat shock and root hair growth (Brost et al., 2019; Gao et al., 2012; Tan et al., 2020). Heterologous expression of CNGC6 in HEK293T cells confirmed its ability to conduct Ca^{2+} (Tan et al., 2020). To elucidate whether CNGC6 is required for eATP-induced activation of PM channel-mediated Ca^{2+} influx, we performed patch-clamp electrophysiology on root epidermal protoplasts. The whole-cell mode of patch clamping was used to measure the net current generated as ions are conducted through PM channels at different transmembrane voltages. The results were reported as the overall current/voltage (*I*/*V*) relationship. In wild-type cells, the addition of 300 μM eATP induced an inward current that was significantly greater than under control conditions (Figure 3a). The mean reversal voltage of the whole-cell current shifted from -54.4 ± 7.5 mV (−ATP, $n = 4$) to -39.8 ± 4.4 mV (+ATP, $n = 4$), approximately a 15-mV positive shift consistent with increased Ca^{2+} influx and far from the equilibrium potential for K^+ (−79 mV). However, as the shift was towards the equilibrium potential for Cl^- (−28 mV), a further test was undertaken. Addition of Gd^{3+} as a blocker of PM-localized Ca^{2+} channels significantly inhibited the eATP-induced current (Figure 3a). Gd^{3+} is ineffective against the root epidermal PM eATP-induced anion conductance (Wang et al., 2019), further supporting the Ca^{2+} permeability of the conductance reported here. This eATP-induced inward current therefore appears competent to increase $[Ca^{2+}]_{cyt}$ at resting membrane voltage (inside negative). In contrast, *cngc6-3* mutant plants failed to respond to 300 μM eATP (Figure 3b). This result suggests that CNGC6 functions as a Ca^{2+}-permeable channel in response to eATP.

ATP-induced MAPK activation and gene expression are defective in *cngc6* mutant plants

Previous studies reported that eATP triggers the activation of MAPKs and a transcriptional response, which are fully dependent on a functional P2K1 (Chen et al., 2017; Choi et al., 2014). Given that CNGC6 participates in eATP

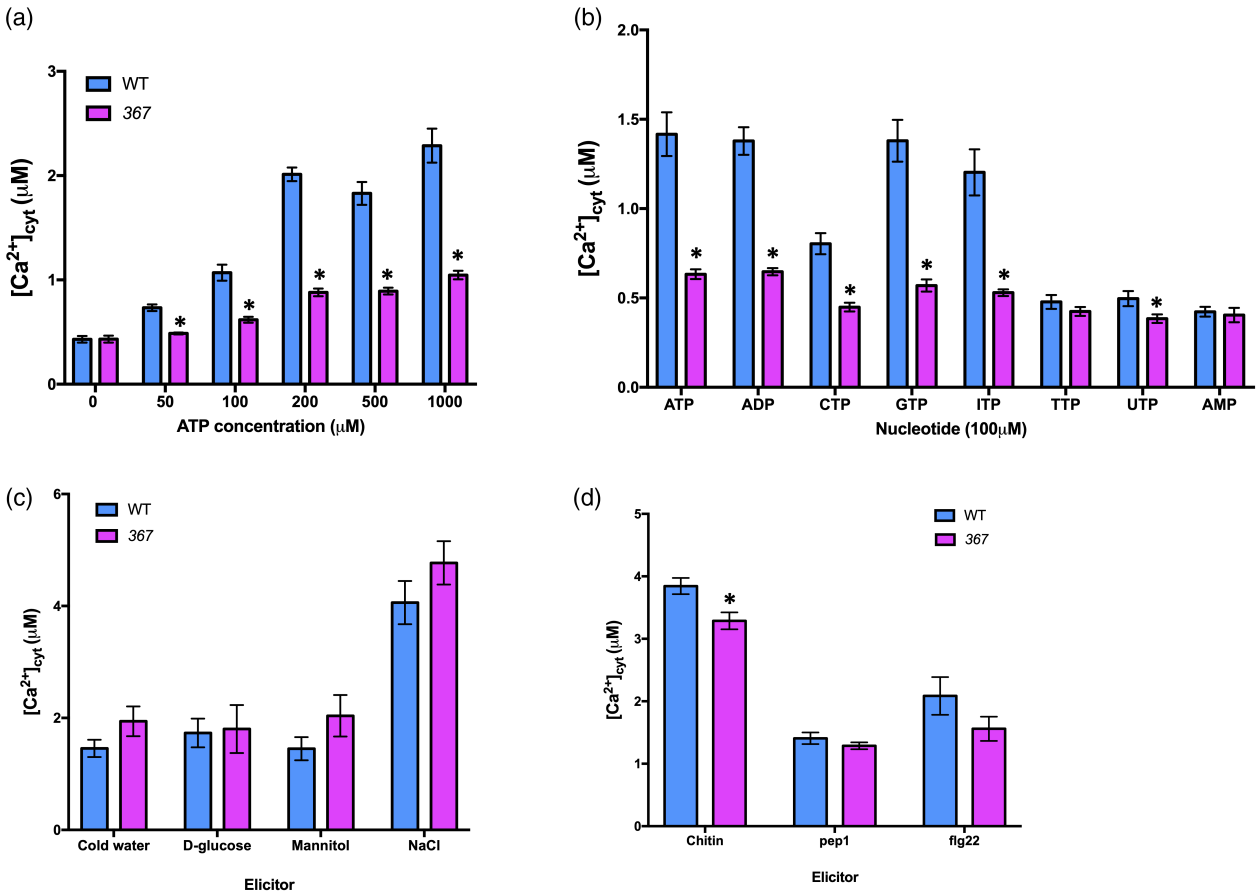

Figure 1. *367* mutant plants show defects in the calcium response to extracellular ATP (eATP) and various nucleotides.
(a) The *367* mutant is impaired in eATP-induced calcium response.
(b) The calcium response to different nucleotides was defective in the *367* mutant.
(c) Abiotic stresses-induced calcium responses in the *367* mutant are comparable to those of wild type (Col-0) (ice-cold water, 300 mM NaCl, 4% D-glucose, and 300 mM mannitol).
(d) The calcium response to chitin is slightly lower in *367* mutant plants (100 nM flg22, 100 nM Pep1, and 100 μg ml^{-1} chitin). The bar graph indicates the integrated calcium concentration in response to ATP addition for 300 sec. Data are presented as mean ± standard error (SE), $n = 8$ in (a, b), $n = 6$ in (c, d). Asterisks indicate a significant difference between wild-type (Col-0) and *367* mutant plants ($P < 0.05$, analysis of variance). Experiments were repeated at least three times with similar results.

signaling (Figure 1), we examined these phenotypes in *cngc6-3* mutant plants. The addition of eATP resulted in a significant reduction in the phosphorylation of MPK3/6 in *cngc6-3* mutant plants as measured 5 and 15 min after eATP addition, while strong activation of MPK3/6 was seen in wild-type plants (Figure 4a). The phosphorylation of MPK3/6 in *cngc6-3* mutant plants was similar to that seen using *p2k1-3* mutant plants (Figure 4a).

Previously, it was shown that eATP addition strongly induced expression of *zinc-finger transcription factor ZAT10*, *bHLH transcription factor MYC2*, and *calcium-dependent protein kinase 28* (*CPK28*) genes (Choi et al., 2014). Consistent with this report, we also found that these genes were strongly upregulated in wild-type plants 30 min after ATP addition, whereas their expression was only slightly enhanced in *cngc6-3* mutant plants (Figure 4b,c). Therefore, in addition to showing defects in the early $[Ca^{2+}]_{cyt}$ response to eATP addition, *cngc6-3* mutant plants are also defective in the later responses of MAPK activation and gene transcription (Figure 4).

CNGC6 plays a role in plant immunity

Previous studies reported that both *P2K1* and *P2K2* are positive regulators of plant immunity against the bacterial pathogen *P. syringae* (Chen et al., 2017; Pham et al., 2020). Previous reports also implicated both *CNGC2* and *CNGC4* in pathogen defense (Chin et al., 2013; Tian et al., 2019), while both *CNGC11* and *CNGC12* are positive regulators of resistance gene-mediated pathogen responses (Yoshioka et al., 2006). In order to test the role of *CNGC6* in plant immunity, we examined plant susceptibility to *P. syringae* upon flood inoculation. Arabidopsis *salicylic acid*

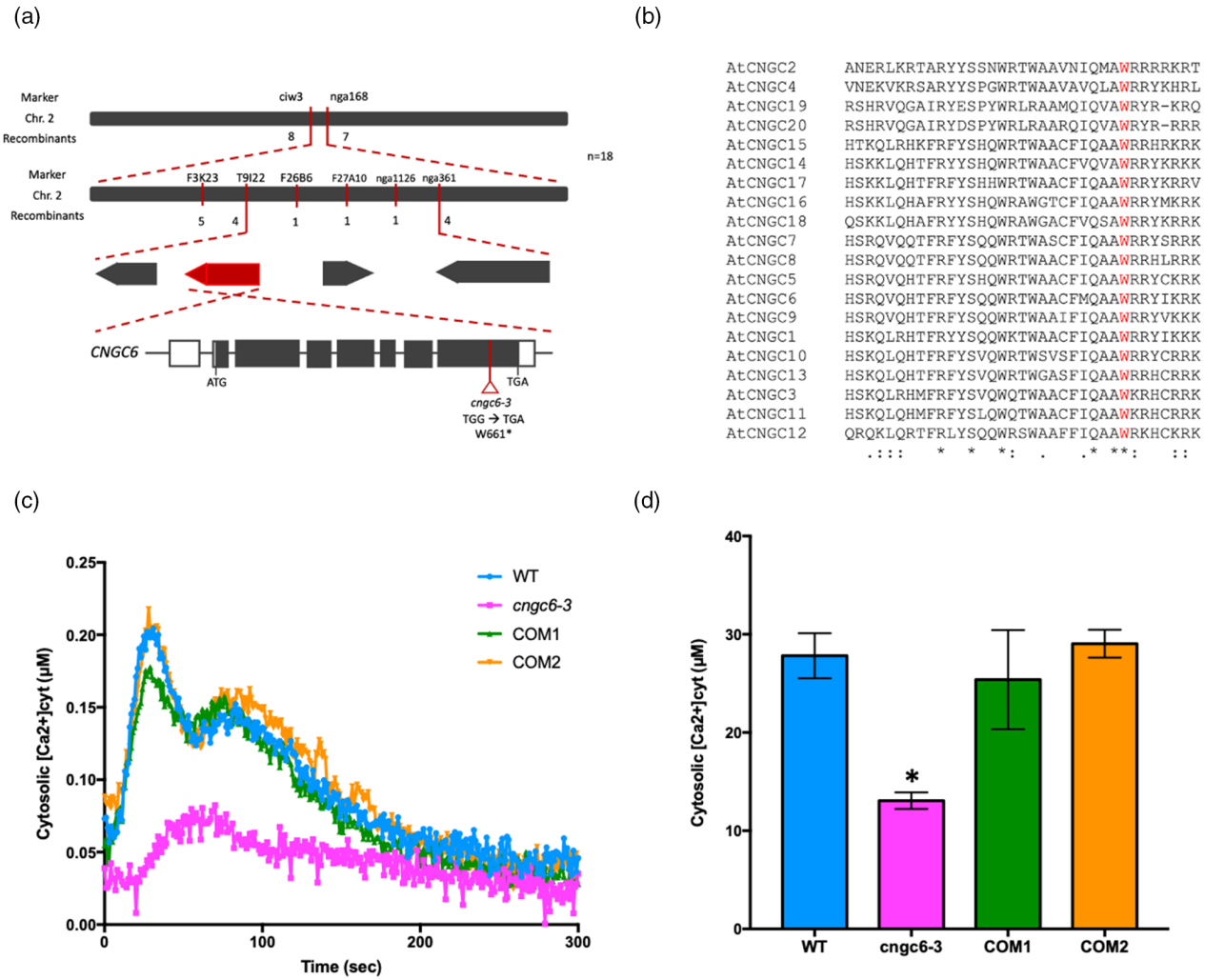

Figure 2. Mutation in *CNGC6* is responsible for the *367* phenotype.
(a) Cartoon showing the genomic structure of *CNGC6*. The open triangle indicates the position of the mutation in mutant *cngc6-3* (TGG → TGA; W661*). The asterisk indicates a stop codon.
(b) CNGC6^{W661} is conserved in the CNGC protein family. Sequence alignment of 20 CNGCs was performed in Clustal Omega (https://www.ebi.ac.uk/Tools/msa/clustalo/). The conserved residue CNGC6^{W661} is marked in red. Asterisks indicate fully conserved residues. Colons indicate highly conserved residues. Dots indicate low conserved residues.
(c, d) $[Ca^{2+}]_{cyt}$ elevation in response to 100 μM ATP for 300 sec in *cngc6-3* mutant plants complemented by *pCNGC6:CNGC6* expression (COM). (c) The kinetics of $[Ca^{2+}]_{cyt}$ in WT, *cngc6-3*, and two COM lines. Each line graph represents an average of four seedlings of each genotype. (d) The bar graph shows the integrated calcium concentration. Data are shown as mean ± standard error (SE) (n = 4). Asterisks indicate a significant difference between wild-type (Col-0) and *367* mutant plants ($P < 0.05$, analysis of variance). Experiments were repeated at least three times with similar results.

induction-deficient 2 (*sid2*) mutant plants were used as the susceptible control (Wildermuth et al., 2001). The degree of bacterial colonization was initially estimated by bioluminescence and subsequently quantified by plate counting. As shown in Figure 5, both *cngc6-3* and *sid2* mutant plants were considerably more susceptible to the pathogen than wild-type plants (Figure 5). In contrast, the *CNGC6* complemented line showed a similar level of infection to that of wild-type plants (Figure 5). These results suggest that CNGC6 is a critical component required for the plant pathogen defense.

DISCUSSION

As is the case in animals, previous studies had clearly shown that an increase in $[Ca^{2+}]_{cyt}$ levels was among the first measurable cellular responses to eATP addition (Choi et al., 2014). In animal systems, eATP triggers the $[Ca^{2+}]_{cyt}$ increase through the action of either P2X-gated ion channels or P2Y G-coupled protein receptors (Burnstock, 2006a). Binding of ATP to P2X receptors induces a channel conformation change, allowing Ca^{2+} influx into cells (Coddou et al., 2011). In contrast, P2Y receptor activation of G-

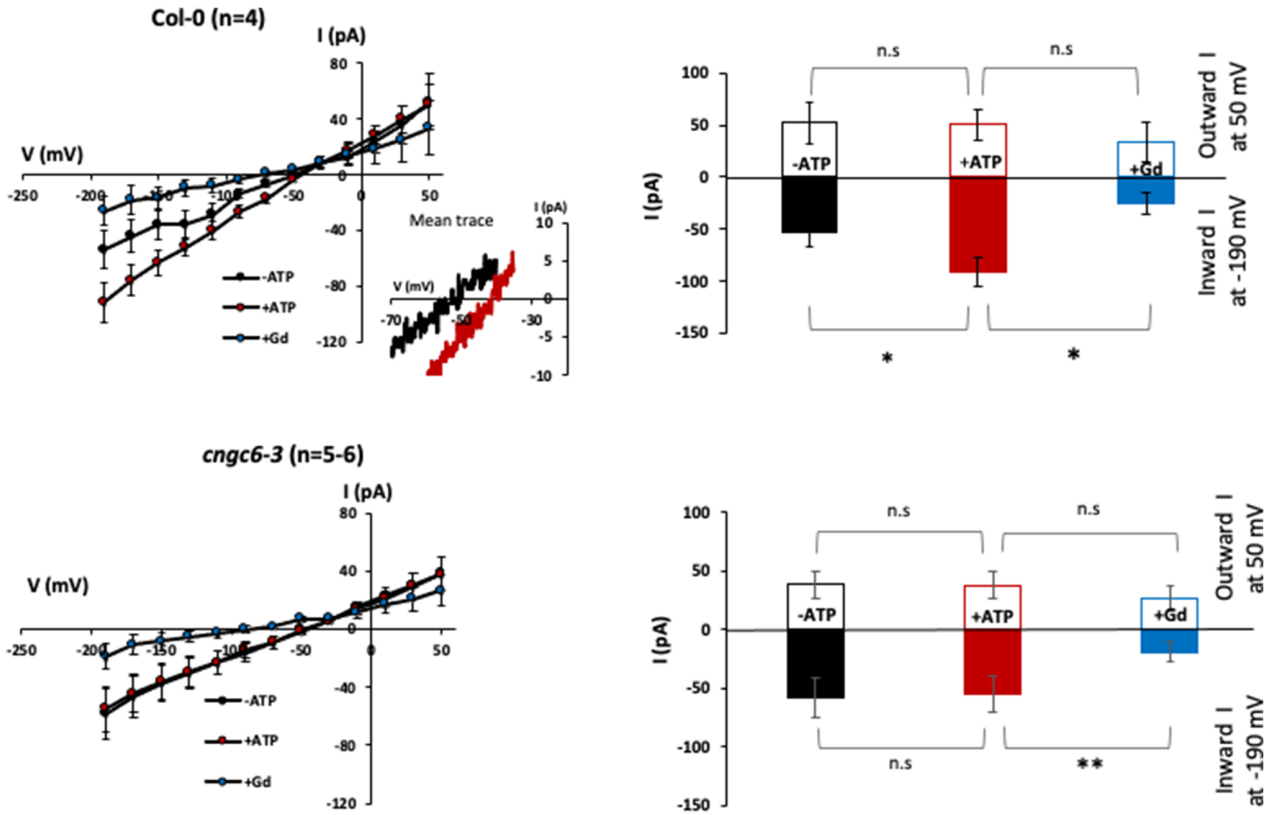

Figure 3. *cngc6-3* failed to support K^+ and Ca^{2+} currents in the root epidermal cell plasma membrane in response to exogenous ATP.
(a) Left panel: Whole-cell current/voltage (*I*/*V*) relationships of wild type (Col-0) in control conditions (no extracellular ATP [−eATP]), after addition of 300 μM eATP (+ATP), and after further addition of 100 μM Gd^{3+} as a calcium channel blocker. eATP activation was observed 30 sec to 3 min after addition. Data are presented as mean ± standard error (SE) of current (n = 4). Inset panel: Mean current traces for −ATP (black) and +ATP (red). Right panel: Comparison of the inward currents at −190 mV (solid bars) and the outward currents at +50 mV (open bars) before and after eATP addition and in the presence of Gd^{3+}. $*P < 0.05$; $**P < 0.01$; n.s, not significant (Student's *t*-test).
(b) As (a) but for the *cngc6-3* mutant (n = 5–6). *cngc6-3* failed to respond to eATP even with an extended observation period of 10 min.

protein signaling networks triggers Ca^{2+} release from the endoplasmic reticulum raising $[Ca^{2+}]_{cyt}$ (Berridge, 2009). In contrast, little is known about the molecular events responsible for eATP-induced $[Ca^{2+}]_{cyt}$ elevation in plants.

The addition of eATP leads to rapid activation of PM HACC conductances, which requires P2K1 (Wang et al., 2018). Our discovery of the critical importance of CNGC6 to the eATP-induced $[Ca^{2+}]_{cyt}$ response is consistent with the previous finding that eATP induces HACC activity (Figure 3) and clearly implicates CNGC family members as key mediators of the eATP-induced $[Ca^{2+}]_{cyt}$ response (Wang et al., 2019). While *p2k1-3* mutant plants show no eATP-mediated $[Ca^{2+}]_{cyt}$ influx (Choi et al., 2014), *cngc6* mutant plants are partially defective in this response with a monophasic increase of about 80 sec (Figure 2c; Figure S2). In the case of ANNEXIN1, loss of ANNEXIN1 significantly reduced the calcium response to eATP in roots, but *ann1* mutant plants still showed a biphasic increase (Mohammad-Sidik et al., 2021). This suggests that CNGC6 is likely not solely responsible for the normal eATP-mediated biphasic $[Ca^{2+}]_{cyt}$ influx and other CNGCs or other channels, including ANNEXIN1, contribute to this $[Ca^{2+}]_{cyt}$ elevation. Indeed, CNGCs are known to work as heteromeric channel complexes, containing more than one CNGC family member (Zhong et al., 2002). Given that the Arabidopsis genome encodes 20 CNGC proteins, the probability of some functional redundancy is high (Maser et al., 2001). For example, it was previously reported that CNGC6, CNGC9, and CNGC14 or CNGC5, CNGC6, and CNGC9 function redundantly as $[Ca^{2+}]_{cyt}$ channels in root hair growth (Brost et al., 2019; Tan et al., 2020). Therefore, one possibility is that other CNGCs act together with CNGC6 in mediating the eATP-induced $[Ca^{2+}]_{cyt}$ response. However, CNGC14 can be excluded from the candidate list, based on the fact that loss of CNGC14 function did not affect the $[Ca^{2+}]_{cyt}$ response to eATP (Shih et al., 2015). The recent discovery of CNGC2 and CNGC4 involvement in eATP-promoted ion influx in the pollen (Wu et al., 2021) is consistent with the hypothesis. However, further studies are needed to unravel whether these CNGC Ca^{2+} channels work together in plant purinergic signaling.

Plants are able to detect DAMP signals by specific pattern recognition receptors (e.g., P2K receptors) (Bigeard

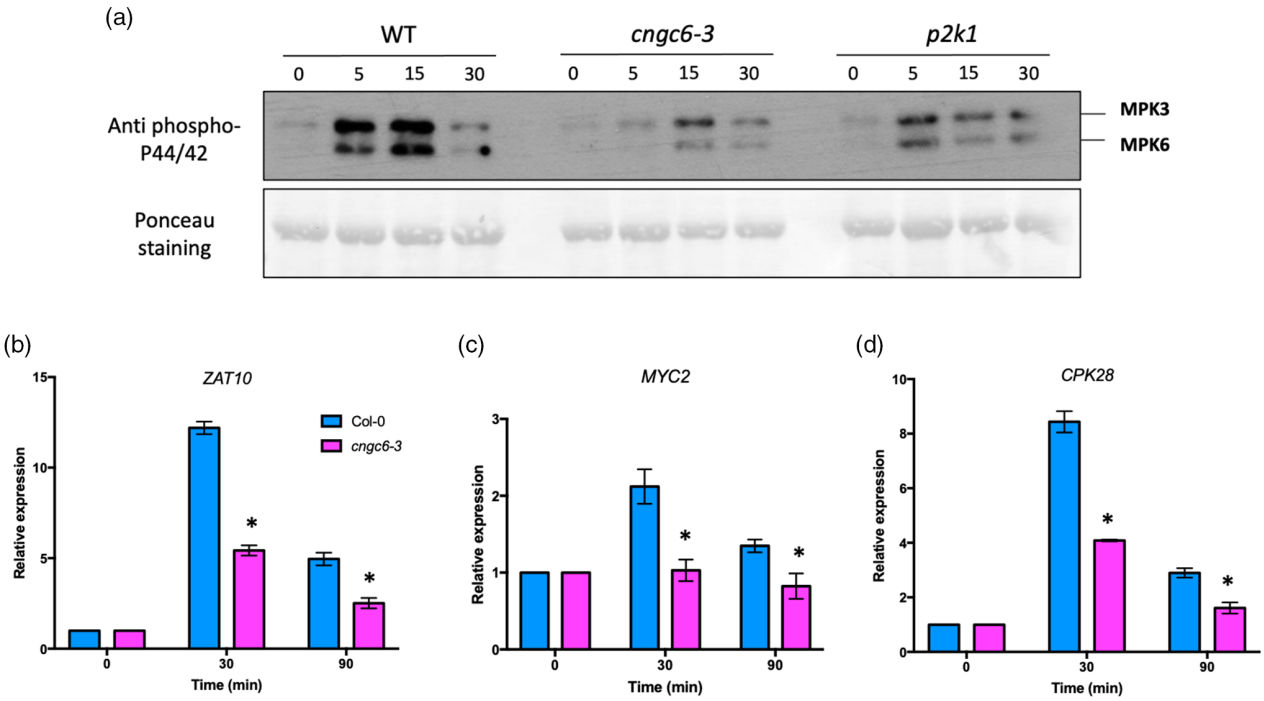

Figure 4. Extracellular ATP (eATP)-induced downstream responses are defective in *cngc6-3* mutant plants.
(a) MPK3 and MPK6 phosphorylation in response to 200 μM eATP is weaker in *cngc6-3* mutant plants compared with wild-type plants. Phosphorylation of MPK3 and MPK6 was detected using an antibody against phospho-p44/p42 MAPK (top). Ponceau S staining was used as a loading control.
(b–d) Col-0 was used as a control to compare with *cngc6-3*. eATP-treated seedlings were collected for qRT-PCR analysis. Expression levels of *ZAT10* (b), *MYC2* (c), and *CPK28* (d) were normalized against the *SAND* reference gene. The results are relative to expression levels of mock-treated plants (set as 1). Bar graphs are presented as mean ± standard error (SE, $n = 3$ biological replicates). Asterisks indicate statistically significant differences between wild type (Col-0) and *cngc6-3* at the same time points (*$P < 0.05$, Student's *t*-test).

et al., 2015; Choi et al., 2014). Moreover, recognition of DAMP signals also activates immune responses (Yamaguchi and Huffaker, 2011). eATP, which is defined as a DAMP, has been shown to regulate the plant response to pathogens (Chivasa et al., 2009; Demidchik et al., 2009; Jewell et al., 2019; Tanaka et al., 2014). Previously various components of eATP signaling have been implicated in plant immunity, including JA signaling and P2K receptors (Balague et al., 2017; Jewell et al., 2019; Pham et al., 2020; Tripathi et al., 2018). Pham et al. (2020) recently showed that P2K1 and P2K2 are required for plant pathogen resistance, in which activation of P2K1 leads to the transphosphorylation of P2K2 and the activation of defense-related downstream signaling components. Thus, plants activate a cascade of ATP-related intracellular events, such as increases in $[Ca^{2+}]_{cyt}$, MAPK phosphorylation, and gene expression (encoding, e.g., MYCs, CPKs, and ZATs), resulting in the activation of pathogen resistance (Figure 4) (Choi et al., 2014; Pham et al., 2020). To date, several members CNGC family members were reported to function in plant pathogen defense including CNGC2 (Chin et al., 2013; Clough et al., 2000), CNGC4 (Chin et al., 2013; Tian et al., 2019), CNGC11/CNGC12 (Yoshioka et al., 2006), CNGC19 (Jogawat et al., 2020), and CNGC20 (Yu et al., 2019). However, none had previously been directly implicated in purinergic signaling. We show here that CNGC6 is involved in P2K innate immunity (Figures 1, 4, and 5), indicating that CNGC6 is likely involved in eATP-dependent plant resistance to pathogens. Taken together, it suggests that CNGC6 acts downstream of the P2K1/P2K2 receptor complex. However, given that Arabidopsis CNGCs are activated directly by cNMPs (Ali et al., 2007; Gao et al., 2012), further analysis is needed to determine whether P2K receptors directly regulate CNGC6 activity or do so indirectly by modulating other cellular processes.

EXPERIMENTAL PROCEDURES

Plant materials and growth conditions

Aequorin-transformed Arabidopsis (Columbia [Col-0] ecotype) and a T-DNA insertion line of *cngc6* (Salk_042207; *cngc6-1*) were crossed to obtain the aequorin transgenic *cngc6-1* line. T-DNA insertion was confirmed by PCR-based genotyping (Table S1). The EMS-induced mutant *cngc6-3* was backcrossed with the Col-0 aequorin transgenic line three times (BC_3F_3). *cngc6-1* and *cngc6-3* were crossed together to obtain the F_1 generation for genetic analysis. These backcrossed lines were then used for phenotyping. Arabidopsis seeds were sown onto half-strength Murashige and Skoog (MS) medium containing 1% (w/v) sucrose, 1% (w/v) agar, and 0.5% (w/v) MES (pH 5.7). After cold treatment for 3 days, the plates were placed vertically in a growth chamber (16 h light/8 h

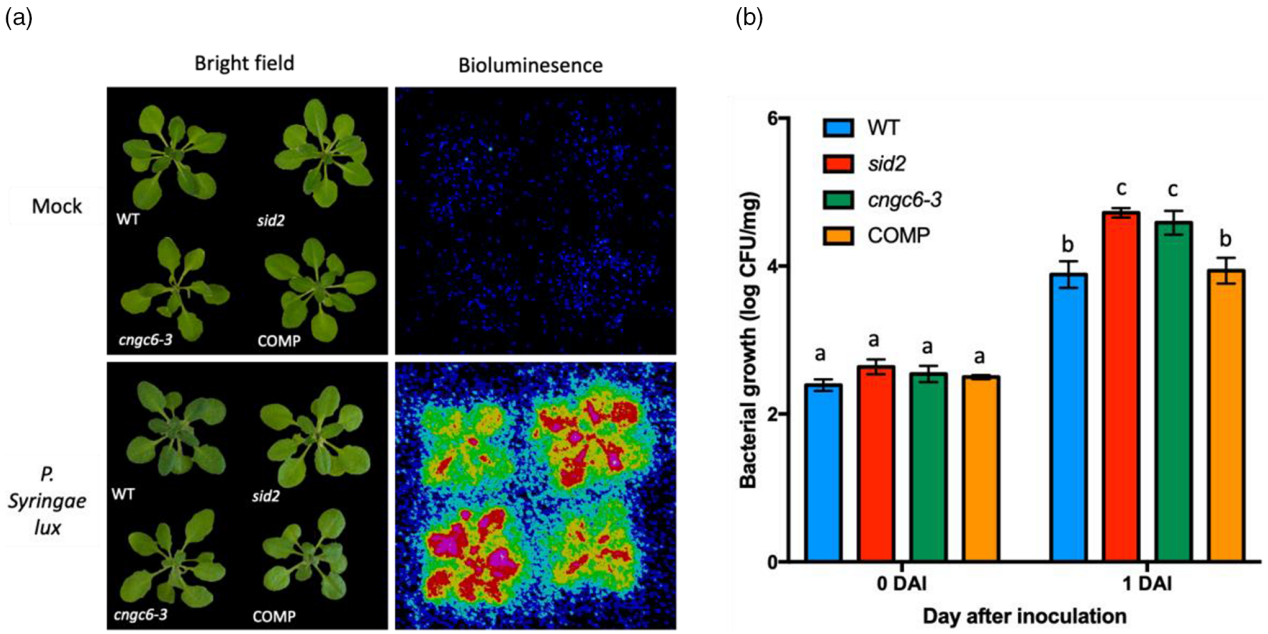

Figure 5. CNGC6 plays a critical role in plant resistance to *Pseudomonas syringae* DC3000.
Wild-type (Col-0) and *sid2* mutant seedlings were used as controls to compare with *cngc6-3* mutant and *pCNGC6:CNGC6* complementation lines (COM). Three-week-old plants were flood-inoculated with *P. syringae* DC3000 lux suspension (OD_{600} = 0.002) containing 0.025% (v/v) Silwet L-77.
(a) At 1 days after inoculation (DAI), bright-field photographs were taken with a normal camera while bioluminescence images were taken using a CCD camera to detect bacterial colonization.
(b) Bacterial colonization by plate counting. Bacterial growth expressed as log(colony forming units [CFU]) was normalized against sample weight. Values are presented as mean ± standard error (SE, $n = 3$ biological replicates). Lowercase letters over bars indicate significantly different means ($P < 0.05$, Student's *t*-test). The experiments were repeated at least three times with similar results.

dark cycle, 22°C, 100 E cm^{-2} sec^{-1} light intensity). For other experiments, 10-day-old seedlings were grown in Sunshine soil (Premier Tech Horticulture, Quebec, Canada) in a growth chamber (12 h light/12 h dark cycle, 22°C, 70% humidity, and 150 E cm^{-2} sec^{-1} light intensity).

Calcium assays

Five- or six-day-old seedlings were individually transferred to a 96-well-plate and incubated in 50 μl reconstitution buffer containing 10 mM $CaCl_2$, 10 μM coelenterazine (CTZ; NanoLight Technology, Pinetop, AZ, USA), and 2 mM MES (pH 5.7) overnight at room temperature in the dark. The next day, 50 μl of 2× treatment solution was applied to each well and the luminescence produced was monitored using an image-intensified CCD camera (Photek216; Photek, Ltd., Lancaster, PA, USA) for 300 sec. Total aequorin levels were estimated by adding 100 μl of discharging buffer containing 2 M $CaCl_2$ and 20% (v/v) ethanol and monitored for an additional 300 sec. The calcium concentrations were converted from photon counting data (Knight et al., 1996). All experiments were performed independently at least three times with similar results. Figures show the converted histogram from each recorded kinetics of the $[Ca^{2+}]_{cyt}$ response during treatments.

Chemical reagents

All chemicals were purchased from Sigma-Aldrich (St. Louis, MO, USA) except if mentioned otherwise. Nucleotide stock solutions (100 mM) in 50 mM MES buffer (pH 5.7) were prepared. Flg22 and Pep1 (GenScript USA, Inc., Piscataway, NJ, USA) stock solutions (1 mM) in dimethylsulfoxide were prepared and kept at −80°C prior to use. Chitin (Sigma, St. Louis, MO, USA) solution (100 μg ml^{-1}) was prepared fresh prior to use.

Mutagenesis and mutant screening

The original *cngc6-3* mutant plant was identified by screening an EMS-mutagenized library derived from *A. thaliana* expressing aequorin (Col-0 background) as described by Choi et al. (2014). Briefly, 5-day-old individual M_2 generation seedlings were transferred into a 96-well plate to monitor the response to the application of 100 μM ATP. Mutants exhibiting a lower cytoplasmic calcium response were selected and grown to test the next generation. M_3 generation seedlings were further tested with the same procedure. In this screen, 2× discharging buffer (20% EtOH, 1 M $CaCl_2$) was applied after ATP treatment to obtain the total light intensity from aequorin expressed in each plant. Discharge data were used to identify plants showing a reduced cytoplasmic calcium response due to a mutation in aequorin. Lastly, the response of the *cngc6-3* mutant plants to ATP was tested by applying an increasing concentration (10, 50, 100, 200, 500, and 1000 μM) of ATP. In addition, we tested the *cngc6-3* mutant plants for the specificity of their defect by applying a variety of known cytoplasmic calcium elicitors/treatments (e.g., 100 μM of ATP, ADP, AMP, GTP, ITP, CTP, TTP, and UTP; 100 nM of flg22 and Pep1, 100 μg ml^{-1} chitin; ice-cold water; 5% D-glucose; 300 mM NaCl and mannitol).

Map-based cloning

The *cngc6-3* mutant plants were crossed with Landsberg *erecta* plants expressing aequorin to generate the mapping population.

The BC_1F_2 plants exhibiting the mutant phenotype were grown further for mapping of *cngc6-3*. Two true leaves from each screened plant were harvested for genomic DNA extraction (DNeasy Plant Mini kit; Qiagen, Hilden, Germany). A region of chromosome 2 was identified as co-segregating with the mutant phenotype. The region between the F26B6 and nga1126 markers with a recombinant frequency of 0.97 was identified as co-segregating with the mutant phenotype. The primers used are listed in Table S3.

Whole-genome sequencing

The mutant *cngc6-3* was backcrossed three times with wild-type Col-0, and homozygous lines (BC_3F_3) all exhibiting the mutant phenotype were used for WGS. Homozygous lines showing a wild-type phenotype from the same backcross line BC_3F_3 were also prepared as an internal reference for sequencing. Single leaves from 29 and 44 individual mutant and wild-type 14-day-old seedlings, respectively, were pooled and genomic DNA was extracted using the DNeasy plant mini kit (Qiagen). WGS was carried out by the DNA Core Facility of the University of Missouri (https://dnacore.missouri.edu) to detect single base mutations. A total of 2.4 μg of genomic DNA was prepared for 350 bp insert size TruSeq library construction. Sequencing was done on a NextSeq 500 system (Illumina, San Diego, CA, USA) (100× coverage). Reads were aligned back to the TAIR10 version of the Arabidopsis genome using Bowtie version 2 (Langmead and Salzberg, 2012). Sam and output-pileup files were generated using Samtools version 0.1.7 (Li et al., 2009). The output-pileup files were converted to NGM emap files using the Next-generation EMS mutation mapping web tool (http://142.150.215.220/ngm/), which were then analyzed for single nucleotide polymorphisms as previously described (Burnstock, 1972).

Plasmid construction and plant transformation

CNGC6 genomic DNA including the 1.5-kb upstream sequence was amplified with primers attB1 and attB2. The PCR product was then inserted into the pDONR-Zeo vector through BP reaction and then into the pGWB1 vector through LR reaction. The pGWB1-CNGC6 construct was then introduced by electroporation into *Agrobacterium tumefaciens* strain GV3101, which was subsequently transformed into *cngc6-3* mutant plants using the floral dip method (Zhang et al., 2006). Transgenic plants were selected on MS medium with 20 mg L^{-1} hygromycin. T_2 generation plants were used for these experiments. The primers used are listed in Table S4.

Patch-clamp electrophysiology assay

Root tips (2–3 mm) were excised from 7- to 13-day-old Col-0 and *cngc6-3* plants. Tips were incubated in the dark at room temperature in 1% (w/v) cellulysin (Calbiochem, San Diego, CA, USA), 1% (w/v) cellulase RS (Yakult Honsha, Tokyo, Japan), 0.1% (w/v) pectolyase Y-23 (Yakult Honsha), 0.1% (w/v) bovine serum albumin, 10 mM $CaCl_2$, 10 mM KCl, 2 mM $MgCl_2$, 2 mM MES, and 165 mM D-sorbitol (pH 5.6) with Tris. After filtering at 40 μm, protoplasts were washed twice with holding buffer (0.2 mM $CaCl_2$, 0.1 mM KCl, and 10 mM MES-Tris [pH 5.6] brought to 280 mosmol L^{-1} with D-sorbitol) at 4 . Protoplasts were suspended in holding buffer and stored on ice in the dark. After using the N9093 epidermal-specific green fluorescent protein reporter line to establish the isolation protocol (Wang et al., 2019), protoplast origin was confirmed by direct observation of the genotypes listed above for testing. The apparatus was as described by Demidchik et al. (2002). After a gigaohm seal was formed in the cell-attached configuration, the whole-cell configuration was achieved by gentle suction and whole-cell currents were recorded after at least 12 min. A ramp protocol from +50 to −190 mV (−200 μV sec^{-1}) with a holding potential at −35 mV (corrected for liquid junction potential) was used. Bath solution contained 50 mM $CaCl_2$, 1 mM KCl, and 10 mM MES-Tris (pH 5.6). The pipette solution contained 5 mM $BaCl_2$, 20 mM KCl, and 10 mM HEPES-Tris (pH 7.5). The osmolarity of bath and pipette solutions was adjusted to 280 and 290 mosmol L^{-1}, respectively, with D-sorbitol. Ionic strength was determined using the calculator integrated in the 'Calcium.exe' program (Fohr et al., 1993). Ion activities were calculated using GEOCHEM (Parker et al., 1994). Equilibrium potentials were calculated using the Nernst equation.

RNA isolation and quantitative real-time PCR

Ten-day-old seedlings of Col-0, *cngc6-1*, or *cngc6-3* were collected and RNA was extracted using TRIzol and the Direct-zol™ RNA miniprep kit (Zymo Research, Irvine, CA, USA). Two micrograms of RNA was used to synthesize cDNA using M-MLV reverse transcriptase (Promega, Madison, WI, USA). These cDNAs were then used for real-time PCR (RT-PCR). The total of 10 μl reaction buffer consisted of 3 μl cDNA, 5 μl PowerUP™ SYBR Green (Applied Biosystems, Waltham, MA, USA), 0.5 μl of each primer, and remaining 1 μl is added water. The reaction was run using an ABI 7500 Real-time PCR system (Applied Biosystems). Transcript levels were normalized against the expression of *SAND* (At2g28390) or *UBQ10* (At4g05320). The primers used are listed in Table S4.

MAPK phosphorylation

Leaf disks from 2- or 3-week-old plants were incubated in 5 mM MES buffer (pH 5.7) at room temperature overnight. After treatment with 200 μM ATP for 0, 5, 15, and 30 min, the samples were homogenized, and the total protein was extracted with protein extraction buffer (100 mM Tris-HCl [pH 7.5], 300 mM NaCl, 2 mM EDTA [pH 8.0], 1% Triton X-100, 10% glycerol, and protease inhibitor). The extracted proteins were mixed with 5× SDS loading buffer (10% SDS, 50% glycerol, 0.01% bromophenol blue, 10% β-mercaptoethanol, 0.3 M Tris-HCl [pH 6.0]) and boiled for 5–10 min. The total proteins were separated by 10% SDS-PAGE and transferred to PVDF membrane. The membrane was then blocked in 5% skim milk in TBST buffer (50 mM Tris-HCl [pH 7.4], 150 mM NaCl, 0.1% Tween-20) and incubated with rabbit anti-phospho-p44/p42 MAPK antibody (Cell Signaling Technology, Danvers, MA, USA), followed by washing with TBST and incubation with HRP-conjugated goat anti-rabbit IgG (Abcam, Cambridge, UK).

Bacterial inoculation assay

The assay was modified from the *P. syringae* flood inoculation method (Pham et al., 2020). Three-week-old Arabidopsis seedlings grown in MS medium were placed into a 40-ml suspension of *P. syringae* pv. *tomato* DC3000 Lux (OD_{600} = 0.002) in sterile water containing 10 mM $MgCl_2$ and 0.025% Silwet L-77 (v/v) for 2–3 min. The suspension was decanted, and the plants were blotted dry and then placed into a growth chamber. One day after inoculation, the seedling aerial parts were collected and weighed. Bacterial growth was visualized and analyzed under a CCD camera (Photek 216). The seedling tissue was then washed with sterilized water and ground in 10 mM $MgCl_2$, diluted serially, and dropped onto King B agar plates supplemented with rifampicin and kanamycin. The number of colonies was counted and analyzed after incubation at room temperature for 2 days.

ACKNOWLEDGMENTS

This research was supported by the National Institute of General Medical Sciences of the National Institutes of Health (grant no. R01GM121445), by the Next-Generation BioGreen 21 Program Systems and Synthetic Agrobiotech Center, Rural Development Administration, Republic of Korea (grant no. PJ01325403), and through the third call of the ERA-NET for Coordinating Action in Plant Sciences, with funding from the US National Science Foundation (grant 1826803) and UKRI BBSRC (BB/S004637/1).

CONFLICT OF INTEREST

The authors declare that there is no conflict of interest.

DATA AVAILABILITY STATEMENT

WGS data of mutant *367* can be found at https://osf.io/csq6t/. Other relevant data can be found within the manuscript and its supporting materials.

SUPPORTING INFORMATION

Additional Supporting Information may be found in the online version of this article.

Figure S1. Mutant screening scheme.

Figure S2. *cngc6-1* and *cngc6-3* mutants are allelic.

Figure S3. $[Ca^{2+}]_{cyt}$ response to different nucleotides and elicitors in mutant *367* complemented by expression of native CNGC6.

Figure S4. The *cngc6-3* mutant developmental phenotype.

Table S1. Rough mapping table of mutant *367*.

Table S2. Whole-genome sequencing showing the mutations of *cngc6-3* in a 3.6-Mbp interval on chromosome 2

Table S3. Mapping primers.

Table S4. Primer list.

REFERENCES

Ali, R., Ma, W., Lemtiri-Chlieh, F., Tsaltas, D., Leng, Q., von Bodman, S. *et al.* (2007) Death don't have no mercy and neither does calcium: Arabidopsis CYCLIC NUCLEOTIDE GATED CHANNEL2 and innate immunity. *The Plant Cell*, **19**(3), 1081–1095.

Balague, C., Gouget, A., Bouchez, O., Souriac, C., Haget, N., Boutet-Mercey, S. *et al.* (2017) The *Arabidopsis thaliana* lectin receptor kinase LecRK-I.9 is required for full resistance to *Pseudomonas syringae* and affects jasmonate signalling. *Molecular Plant Pathology*, **18**(7), 937–948.

Berridge, M.J. (2009) Inositol trisphosphate and calcium signalling mechanisms. *Biochimica et Biophysica Acta*, **1793**(6), 933–940.

Bigeard, J., Colcombet, J. & Hirt, H. (2015) Signaling mechanisms in pattern-triggered immunity (PTI). *Molecular Plant*, **8**(4), 521–539.

Brost, C., Studtrucker, T., Reimann, R., Denninger, P., Czekalla, J., Krebs, M. *et al.* (2019) Multiple cyclic nucleotide-gated channels coordinate calcium oscillations and polar growth of root hairs. *The Plant Journal*, **99**(5), 910–923.

Burnstock, G. (1972) Purinergic nerves. *Pharmacological Reviews*, **24**(3), 509–581.

Burnstock, G. (2006a) Pathophysiology and therapeutic potential of purinergic signaling. *Pharmacological Reviews*, **58**(1), 58–86.

Burnstock, G. (2006b) Purinergic signalling. *British Journal of Pharmacology*, **147**(Suppl 1), S172–S181.

Cekic, C. & Linden, J. (2016) Purinergic regulation of the immune system. *Nature Reviews Immunology*, **16**(3), 177–192.

Chen, D., Cao, Y., Li, H., Kim, D., Ahsan, N., Thelen, J. *et al.* (2017) Extracellular ATP elicits DORN1-mediated RBOHD phosphorylation to regulate stomatal aperture. *Nature Communications*, **8**(1), 2265.

Chen, D., Hao, F., Mu, H., Ahsan, N., Thelen, J.J. & Stacey, G. (2021) S-acylation of P2K1 mediates extracellular ATP-induced immune signaling in Arabidopsis. *Nature Communications*, **12**(1), 2750.

Chin, K., DeFalco, T.A., Moeder, W. & Yoshioka, K. (2013) The Arabidopsis cyclic nucleotide-gated ion channels AtCNGC2 and AtCNGC4 work in the same signaling pathway to regulate pathogen defense and floral transition. *Plant Physiology*, **163**(2), 611–624.

Chivasa, S., Murphy, A.M., Hamilton, J.M., Lindsey, K., Carr, J.P. & Slabas, A.R. (2009) Extracellular ATP is a regulator of pathogen defence in plants. *The Plant Journal*, **60**(3), 436–448.

Cho, S.H., Nguyen, C.T., Choi, J. & Stacey, G. (2017) Molecular mechanism of plant recognition of extracellular ATP. *Advances in Experimental Medicine and Biology*, **1051**, 233–253.

Choi, J., Tanaka, K., Cao, Y., Qi, Y., Qiu, J., Liang, Y. *et al.* (2014) Identification of a plant receptor for extracellular ATP. *Science*, **343**(6168), 290–294.

Clark, G. & Roux, S.J. (2018) Role of Ca^{2+} in mediating plant responses to extracellular ATP and ADP. *International Journal of Molecular Sciences*, **19**(11), 3590.

Clark, G., Wu, M., Wat, N., Onyirimba, J., Pham, T., Herz, N. *et al.* (2010) Both the stimulation and inhibition of root hair growth induced by extracellular nucleotides in Arabidopsis are mediated by nitric oxide and reactive oxygen species. *Plant Molecular Biology*, **74**(4–5), 423–435.

Clough, S.J., Fengler, K.A., Yu, I.C., Lippok, B., Smith, R.K. Jr & Bent, A.F. (2000) The Arabidopsis dnd1 "defense, no death" gene encodes a mutated cyclic nucleotide-gated ion channel. *Proceedings of the National Academy of Sciences of the United States of America*, **97**(16), 9323–9328.

Coddou, C., Yan, Z., Obsil, T., Huidobro-Toro, J.P. & Stojilkovic, S.S. (2011) Activation and regulation of purinergic P2X receptor channels. *Pharmacological Reviews*, **63**(3), 641–683.

Demidchik, V., Bowen, H.C., Maathuis, F.J., Shabala, S.N., Tester, M.A., White, P.J. *et al.* (2002) *Arabidopsis thaliana* root non-selective cation channels mediate calcium uptake and are involved in growth. *The Plant Journal*, **32**(5), 799–808.

Demidchik, V., Shabala, S., Isayenkov, S., Cuin, T.A. & Pottosin, I. (2018) Calcium transport across plant membranes: mechanisms and functions. *New Phytologist*, **220**(1), 49–69.

Demidchik, V., Shang, Z., Shin, R., Thompson, E., Rubio, L., Laohavisit, A. *et al.* (2009) Plant extracellular ATP signalling by plasma membrane NADPH oxidase and Ca^{2+} channels. *The Plant Journal*, **58**(6), 903–913.

Dichmann, S., Idzko, M., Zimpfer, U., Hofmann, C., Ferrari, D., Luttmann, W. *et al.* (2000) Adenosine triphosphate-induced oxygen radical production and CD11b up-regulation: Ca(++) mobilization and actin reorganization in human eosinophils. *Blood*, **95**(3), 973–978.

Dodd, A.N., Kudla, J. & Sanders, D. (2010) The language of calcium signaling. *Annual Review of Plant Biology*, **61**, 593–620.

Fohr, K.J., Warchol, W. & Gratzl, M. (1993) Calculation and control of free divalent cations in solutions used for membrane fusion studies. *Methods in Enzymology*, **221**, 149–157.

Gao, F., Han, X., Wu, J., Zheng, S., Shang, Z., Sun, D. *et al.* (2012) A heat-activated calcium-permeable channel–Arabidopsis cyclic nucleotide-gated ion channel 6–is involved in heat shock responses. *The Plant Journal*, **70**(6), 1056–1069.

Gout, E., Bligny, R. & Douce, R. (1992) Regulation of intracellular pH values in higher plant cells. Carbon-13 and phosphorus-31 nuclear magnetic resonance studies. *Journal of Biological Chemistry*, **267**(20), 13903–13909.

Jewell, J.B., Sowders, J.M., He, R., Willis, M.A., Gang, D.R. & Tanaka, K. (2019) Extracellular ATP shapes a defense-related transcriptome both independently and along with other defense signaling pathways. *Plant Physiology*, **179**(3), 1144–1158.

Jogawat, A., Meena, M.K., Kundu, A., Varma, M. & Vadassery, J. (2020) Calcium channel CNGC19 mediates basal defense signaling to regulate colonization by *Piriformospora indica* in Arabidopsis roots. *Journal of Experimental Botany*, **71**(9), 2752–2768.

Khakh, B.S. & Burnstock, G. (2009) The double life of ATP. *Scientific American*, **301**(6), 84–92.

Kim, S.Y., Sivaguru, M. & Stacey, G. (2006) Extracellular ATP in plants. Visualization, localization, and analysis of physiological significance in growth and signaling. *Plant Physiology*, **142**(3), 984–992.

Knight, H., Trewavas, A.J. & Knight, M.R. (1996) Cold calcium signaling in Arabidopsis involves two cellular pools and a change in calcium signature after acclimation. *The Plant Cell*, **8**(3), 489–503.

Kudla, J., Batistic, O. & Hashimoto, K. (2010) Calcium signals: the lead currency of plant information processing. *The Plant Cell*, **22**(3), 541–563.

Langmead, B. & Salzberg, S.L. (2012) Fast gapped-read alignment with Bowtie 2. *Nature Methods*, **9**(4), 357–359.

Laohavisit, A., Shang, Z., Rubio, L., Cuin, T.A., Very, A.A., Wang, A. *et al.* (2012) Arabidopsis annexin1 mediates the radical-activated plasma membrane Ca(2)+- and K+-permeable conductance in root cells. *The Plant Cell*, **24**(4), 1522–1533.

Lemtiri-Chlieh, F., Arold, S.T. & Gehring, C. (2020) Mg^{2+} is a missing link in plant cell Ca^{2+} signalling and homeostasis-a study on *Vicia faba* guard cells. *International Journal of Molecular Sciences*, **21**(11), 3771.

Li, H., Handsaker, B., Wysoker, A., Fennell, T., Ruan, J., Homer, N. *et al.* (2009) The Sequence Alignment/Map format and SAMtools. *Bioinformatics*, **25**(16), 2078–2079.

Maser, P., Thomine, S., Schroeder, J.I., Ward, J.M., Hirschi, K., Sze, H. *et al.* (2001) Phylogenetic relationships within cation transporter families of Arabidopsis. *Plant Physiology*, **126**(4), 1646–1667.

Matthus, E., Sun, J., Wang, L., Bhat, M.G., Mohammad-Sidik, A.B., Wilkins, K.A. *et al.* (2020) DORN1/P2K1 and purino-calcium signalling in plants: making waves with extracellular ATP. *Annals of Botany*, **124**(7), 1227–1242.

McAinsh, M.R. & Pittman, J.K. (2009) Shaping the calcium signature. *New Phytologist*, **181**(2), 275–294.

Mohammad-Sidik, A., Sun, J., Shin, R., Song, Z., Ning, Y., Matthus, E. *et al.* (2021) Annexin 1 is a component of eATP-induced cytosolic calcium elevation in *Arabidopsis thaliana* roots. *International Journal of Molecular Sciences*, **22**(2), 494.

Parker, D.R., Norvell, W.A. & Chaney, R.L. (1994). A chemical specition program for IBM and compatible computers. In: Loeppert, R.H., Paul Schwab, A. & Goldberg, S. (Eds.) *Chemical equilibrium and reaction models*. SSSA Spec Pub No. Madison, WI: Soil Science Society of America.

Pham, A.Q., Cho, S.H., Nguyen, C.T. & Stacey, G. (2020) Arabidopsis lectin receptor kinase P2K2 Is a second plant receptor for extracellular ATP and contributes to innate immunity. *Plant Physiology*, **183**(3), 1364–1375.

Rhett, J.M., Fann, S.A. & Yost, M.J. (2014) Purinergic signaling in early inflammatory events of the foreign body response: modulating extracellular ATP as an enabling technology for engineered implants and tissues. *Tissue Engineering Part B Reviews*, **20**(5), 392–402.

Savio, L.E.B., de Andrade Mello, P., da Silva, C.G. & Coutinho-Silva, R. (2018) The P2X7 receptor in inflammatory diseases: angel or demon? *Frontiers in Pharmacology*, **9**, 52.

Shih, H.W., DePew, C.L., Miller, N.D. & Monshausen, G.B. (2015) The cyclic nucleotide-gated channel CNGC14 regulates root gravitropism in *Arabidopsis thaliana*. *Current Biology*, **25**(23), 3119–3125.

Silva, G., Beierwaltes, W.H. & Garvin, J.L. (2006) Extracellular ATP stimulates NO production in rat thick ascending limb. *Hypertension*, **47**(3), 563–567.

Song, C.J., Steinebrunner, I., Wang, X., Stout, S.C. & Roux, S.J. (2006) Extracellular ATP induces the accumulation of superoxide via NADPH oxidases in Arabidopsis. *Plant Physiology*, **140**(4), 1222–1232.

Tan, Y.Q., Yang, Y., Zhang, A., Fei, C.F., Gu, L.L., Sun, S.J. *et al.* (2020) Three CNGC family members, CNGC5, CNGC6, and CNGC9, are required for constitutive growth of arabidopsis root hairs as Ca^{2+}-permeable channels. *Plant Commun*, **1**(1), 100001.

Tanaka, K., Choi, J., Cao, Y. & Stacey, G. (2014) Extracellular ATP acts as a damage-associated molecular pattern (DAMP) signal in plants. *Frontiers in Plant Science*, **5**, 446.

Tanaka, K., Gilroy, S., Jones, A.M. & Stacey, G. (2010a) Extracellular ATP signaling in plants. *Trends in Cell Biology*, **20**(10), 601–608.

Tanaka, K., Swanson, S.J., Gilroy, S. & Stacey, G. (2010b) Extracellular nucleotides elicit cytosolic free calcium oscillations in Arabidopsis. *Plant Physiology*, **154**(2), 705–719.

Tang, W., Brady, S.R., Sun, Y., Muday, G.K. & Roux, S.J. (2003) Extracellular ATP inhibits root gravitropism at concentrations that inhibit polar auxin transport. *Plant Physiology*, **131**(1), 147–154.

Tian, W., Hou, C., Ren, Z., Wang, C., Zhao, F., Dahlbeck, D. *et al.* (2019) A calmodulin-gated calcium channel links pathogen patterns to plant immunity. *Nature*, **572**(7767), 131–135.

Tripathi, D., Zhang, T., Koo, A.J., Stacey, G. & Tanaka, K. (2018) Extracellular ATP acts on jasmonate signaling to reinforce plant defense. *Plant Physiology*, **176**(1), 511–523.

van der Vliet, A. & Bove, P.F. (2011) Purinergic signaling in wound healing and airway remodeling. *SubCellular Biochemistry*, **55**, 139–157.

Very, A.A. & Sentenac, H. (2002) Cation channels in the Arabidopsis plasma membrane. *Trends in Plant Science*, **7**(4), 168–175.

Vincent, T.R., Avramova, M., Canham, J., Higgins, P., Bilkey, N., Mugford, S.T. *et al.* (2017) Interplay of plasma membrane and vacuolar ion channels, together with BAK1, elicits rapid cytosolic calcium elevations in Arabidopsis during aphid feeding. *The Plant Cell*, **29**(6), 1460–1479.

Wang, F., Jia, J., Wang, Y., Wang, W., Chen, Y., Liu, T. *et al.* (2014) Hyperpolization-activated Ca^{2+} channels in guard cell plasma membrane are involved in extracellular ATP-promoted stomatal opening in *Vicia faba*. *Journal of Plant Physiology*, **171**(14), 1241–1247.

Wang, L., Stacey, G., Leblanc-Fournier, N., Legue, V., Moulia, B. & Davies, J.M. (2019) Early extracellular ATP signaling in Arabidopsis root epidermis: a multi-conductance process. *Frontiers in Plant Science*, **10**, 1064.

Wang, L., Wilkins, K.A. & Davies, J.M. (2018) Arabidopsis DORN1 extracellular ATP receptor; activation of plasma membrane K^+ and Ca^{2+}-permeable conductances. *New Phytologist*, **218**(4), 1301–1304.

Wang, Y.F., Munemasa, S., Nishimura, N., Ren, H.M., Robert, N., Han, M. *et al.* (2013) Identification of cyclic GMP-activated nonselective Ca^{2+}-permeable cation channels and associated CNGC5 and CNGC6 genes in Arabidopsis guard cells. *Plant Physiology*, **163**(2), 578–590.

Weerasinghe, R.R., Swanson, S.J., Okada, S.F., Garrett, M.B., Kim, S.Y., Stacey, G. *et al.* (2009) Touch induces ATP release in Arabidopsis roots that is modulated by the heterotrimeric G-protein complex. *FEBS Letters*, **583**(15), 2521–2526.

White, P.J. & Broadley, M.R. (2003) Calcium in plants. *Annals of Botany*, **92** (4), 487–511.

Wildermuth, M.C., Dewdney, J., Wu, G. & Ausubel, F.M. (2001) Isochorismate synthase is required to synthesize salicylic acid for plant defence. *Nature*, **414**(6863), 562–565.

Wu, S.J. & Wu, J.Y. (2008) Extracellular ATP-induced NO production and its dependence on membrane Ca^{2+} flux in *Salvia miltiorrhiza* hairy roots. *Journal of Experimental Botany*, **59**(14), 4007–4016.

Wu, Y., Qin, B., Feng, K., Yan, R., Kang, E., Liu, T. *et al.* (2018) Extracellular ATP promoted pollen germination and tube growth of *Nicotiana tabacum* through promoting K^+ and Ca^{2+} absorption. *Plant Reproduction*, **31** (4), 399–410.

Wu, Y., Yin, H., Liu, X., Xu, J., Qin, B., Feng, K. *et al.* (2021) P2K1 receptor, heterotrimeric Gα protein and CNGC2/4 are involved in extracellular ATP-promoted ion influx in the pollen of *Arabidopsis thaliana*. *Plants*, **10**(8), 1743.

Yamaguchi, Y. & Huffaker, A. (2011) Endogenous peptide elicitors in higher plants. *Current Opinion in Plant Biology*, **14**(4), 351–357.

Yang, X., Wang, B., Farris, B., Clark, G. & Roux, S.J. (2015) Modulation of root skewing in Arabidopsis by apyrases and extracellular ATP. *Plant and Cell Physiology*, **56**(11), 2197–2206.

Yegutkin, G.G., Mikhailov, A., Samburski, S.S. & Jalkanen, S. (2006) The detection of micromolar pericellular ATP pool on lymphocyte surface by using lymphoid ecto-adenylate kinase as intrinsic ATP sensor. *Molecular Biology of the Cell*, **17**(8), 3378–3385.

Yoshioka, K., Moeder, W., Kang, H.G., Kachroo, P., Masmoudi, K., Berkowitz, G. *et al.* (2006) The chimeric Arabidopsis CYCLIC NUCLEOTIDE-GATED ION CHANNEL11/12 activates multiple pathogen resistance responses. *The Plant Cell*, **18**(3), 747–763.

Yu, X., Xu, G., Li, B., de Souza Vespoli, L., Liu, H., Moeder, W. *et al.* (2019) The receptor kinases BAK1/SERK4 regulate Ca^{2+} channel-mediated cellular homeostasis for cell death containment. *Current Biology*, **29**(22), 3778–3790.e8.

Zhang, X., Henriques, R., Lin, S.S., Niu, Q.W. & Chua, N.H. (2006) Agrobacterium-mediated transformation of *Arabidopsis thaliana* using the floral dip method. *Nature Protocols*, **1**(2), 641–646.

Zhong, H., Molday, L.L., Molday, R.S. & Yau, K.W. (2002) The heteromeric cyclic nucleotide-gated channel adopts a 3A:1B stoichiometry. *Nature*, **420**(6912), 193–198.